Empty Level Structure and Dissociative Electron Attachment Cross Section in (Bromoalkyl)benzenes

Alberto Modelli†

Dipartimento di Chimica "G. Ciamician", Università di Bologna, via Selmi 2, 40126 Bologna, Italy, and Centro Interdipartimentale di Ricerca in Scienze Ambientali (CIRSA), Università di Bologna, via S. Alberto 163, 48100 Ravenna, Italy

Received: April 18, 2005; In Final Form: May 25, 2005

The gas-phase electron transmission (ET) and dissociative electron attachment (DEA) spectra are reported for the series of (bromoalkyl)benzenes $C_6H_5(CH_2)_nBr$ ($n = 0-3$), where the bromine atom is directly bonded to a benzene ring or separated from it by 1−3 CH_2 groups, and the dihalo derivative 1-Br-4-Cl-benzene. The relative DEA cross sections (essentially due to the Br^- fragment) are reported, and the absolute cross sections are also evaluated. HF/6-31G and B3LYP/6-31G* calculations are employed to evaluate the virtual orbital energies (VOEs) for the optimized geometries of the neutral state molecules. The π^* VOEs, scaled with empirical equations, satisfactorily reproduce the corresponding experimental vertical electron attachment energies (VAEs). According to the calculated localization properties, the LUMO (as well as the singly occupied MO of the lowest lying anion state) of $C_6H_5(CH_2)_3Br$ is largely localized on both the benzene ring and the C−Br bond, despite only a small π^*/σ^*_{C-Br} interaction and in contrast to the chlorine analogue where the LUMO is predicted to possess essentially ring π^* character. This would imply a less important role of intramolecular electron transfer in the bromo derivative for production of the halogen negative fragment through dissociation of the first resonant state. The VAEs calculated as the anion/neutral energy difference with the 6-31+G* basis set which includes diffuse functions are relatively close to the experimental values but do not parallel their sequence. In addition the SOMO of some compounds is not described as a valence MO with large π^* character but as a diffuse σ^* MO.

Introduction

Electron−molecule collisions play an important role in various scientific fields, from both theoretical and technological points of view.[1] In particular, dissociative single-electron-transfer reactions in solution

$$RX + e^- \rightarrow R\bullet + X^-$$

(where R• is a neutral organic radical and X^- is a negative fragment) are extensively studied[2−4] processes because of their great relevance in electrochemistry, biochemistry, and photochemistry.

The counterpart of this process in the gas phase is referred to as dissociative electron attachment.[5] As a first step, an isolated molecule can temporarily accept a free electron of proper energy into a vacant molecular orbital (MO) to form an unstable short-lived RX^- anion. Then, when suitable energetic conditions occur, the decay of the temporary molecular anion can follow a dissociative channel which generates a long-lived negative fragment and a neutral radical, in kinetic competition[6] with simple reemission of the extra electron:

$$RX + e^- \rightarrow RX^- \rightarrow R\bullet + X^-$$

An important improvement in the detection and characterization of unstable gas-phase anions was made with the electron transmission spectroscopy (ETS) technique devised by Sanche and Schulz,[7] which is still one of the most suitable means for measuring negative electron affinities (EAs). The ETS technique takes advantage of the sharp variations in the total electron−molecule scattering cross section caused by resonance processes, namely, temporary capture of electrons with appropriate energy and angular momentum into empty MOs.[5] Electron attachment is rapid with respect to nuclear motion, so that temporary anions are formed in the equilibrium geometry of the neutral molecule. The measured vertical attachment energies (VAEs) are the negative of the vertical EAs.

Additional information on temporary negative ion states can be supplied by dissociative electron attachment spectroscopy (DEAS),[5,8] which measures the yield of negative fragments as a function of the incident electron energy, thus revealing possible dissociative decay channels of the molecular anions formed by resonance.

Measurements of DEA cross sections, in conjunction with ETS, provide an important probe for estimating the efficiency of intramolecular electron transfer processes, when an incident electron is first trapped into a localized functional group and then transferred to a remote group (or atom) where bond dissociation with the formation of a negative fragment takes place. Such long-range electron transfer processes play an important role in photochemistry and biochemistry. In addition, systems capable of transmitting variations of charge density between different parts of a molecule are increasingly important in the field of nanoscale technology, i.e., organic conductors, molecular wires, and molecular devices.[9]

† Corresponding author. Telephone: +39 051 2099522. Fax: +39 051 2099456. E-mail: alberto.modeli@unibo.it.

10.1021/jp051991b CCC: $30.25
Published on Web 06/22/2005

We have recently employed ETS and DEAS to study the empty level structure of chloroalkyl derivatives with general formula $R(CH_2)_nCl$, with R = benzene,[10,11] ethene, and ethyne,[12] where the chlorine atom is directly bonded ($n = 0$) to a π-functional or separated by an increasing number of intermediate CH_2 groups. Electron capture into the (π^*) lowest unoccupied MO (LUMO) of these unsaturated chlorohydrocarbons is followed by Cl^- production. Although the magnitude of the DEA cross section is affected by the π-functional, on going from the $-CH_2Cl$ (where the greatest σ^*_{C-Cl}/π^* mixing occurs) to the $-(CH_2)_3Cl$ derivative of each π-system, the Cl^- current decreases by more than 2 orders of magnitude, becoming intermediate between those measured in (saturated) normal and secondary chloroalkanes, where production of the chloride anion derives directly from dissociation of the σ^*_{C-Cl} resonance.

In the analogous series of (bromoalkyl)ethenes the Br^- cross section (always larger than the Cl^- cross section in the chlorine analogues) was also found[13] to decrease with increasing length of the alkyl chain but somewhat less rapidly with respect to the Cl^- yield in the chloroethenes. In fact, a remarkable difference between the two series was found. In 5-Br-1-pentene ($n = 3$) and in longer chain bromoalkenes the LUMO was found to be a σ^*_{C-Br} MO, whereas in the corresponding chloroalkenes the LUMO is a mainly ethene π^* MO. This finding is consistent with the σ^*_{C-Br} and σ^*_{C-Cl} VAEs in the saturated linear haloalkanes (about 1.3 and 2.4 eV, respectively), to be compared with the intermediate π^* VAE (1.73 eV[14]) of ethene. Thus, in the bromoalkenes with $n = 3$ and 4, Br^- production derives mainly from direct dissociation of the σ^*_{C-Br} resonance, whereas in the chlorine counterparts Cl^- production is mainly due to electron capture into the π^* LUMO, followed by intramolecular electron transfer through the alkyl chain.

Here we extend the ET study of the empty level structure and measurements of the DEA cross sections to the (bromoalkyl)benzenes $C_6H_5(CH_2)_nBr$ ($n = 0-3$) from bromobenzene to 1-Br-3-phenylpropane. In addition, 1-Br-4-Cl-benzene is also analyzed, to compare the absolute and relative Br^- and Cl^- cross sections with those of chloro- and bromobenzene and gain insight into the mutual effects produced by the two halogen atoms.

The π^* VAE of benzene (1.12 eV[15]) is slightly lower than the σ^*_{C-Br} VAE (1.3 eV[13]) of the normal bromoalkanes, so that the localization properties of the LUMO in the 1-Br-*n*-phenylalkanes with $n > 2$ could be substantially different from that of their ethene analogues; namely, the LUMO could possess a large benzene π^* character, with a subsequently different DEA mechanism. The ET spectra, interpreted with the support of theoretical calculations, and comparison of the VAEs with the energies of the peaks in the DEA spectra, as well as the relative DEA cross sections, are expected to provide more insight into the empty level structure and the dissociative mechanism (i.e., the role played by the π^* and σ^* resonances) in the (bromoalkyl)benzenes.

A theoretical approach adequate for describing the energetics of unstable anion states involves difficulties not encountered for neutral or cation states. The most correct approach is, in principle, the calculation of the total scattering cross section with the use of continuum functions, although complications arise from an accurate description of the electron−molecule interactions.[16]

The first VAE can be obtained as the energy difference between the lowest lying anion and the neutral state (both with the optimized geometry of the neutral species), but the description of resonance anion states (unstable with respect to electron loss) with standard bound state methods poses a serious problem. The use of a finite basis set formed with (Gaussian) functions has the effect of confining the system within a box, accounting in some way for the fact that during a resonance process the extra electron is confined to the molecule by a potential barrier.[17] However, a proper description of the spatially diffuse electron distributions of anions requires a basis set with diffuse functions.[18,19] On the other hand, as the basis set is expanded, the wave function ultimately describes a neutral molecule and an unbound electron in the continuum,[12,17,20,21] since this is the state of minimum energy. The choice of a basis set which gives a satisfactory description of the energy and nature of resonance processes is therefore a delicate task.[22]

CHART 1

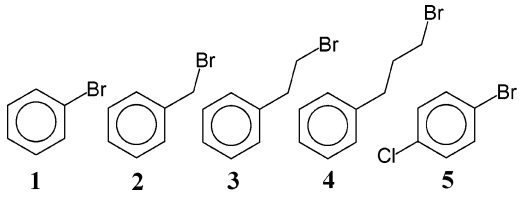

The Koopmans' theorem (KT) approximation[23] neglects correlation and relaxation effects. However, Chen and Gallup[24] and Staley and Strnad[21] demonstrated the occurrence of good linear correlations between the $\pi^*_{C=C}$ VAEs measured in a large number of alkenes and benzenoid hydrocarbons and the corresponding virtual orbital energies (VOEs) of the neutral molecules obtained with simple KT-HF calculations, using basis sets which do not include diffuse functions. We have recently shown[12] that also the neutral state π^* VOEs obtained with B3LYP/6-31G* calculations supply a good linear correlation with the corresponding VAEs measured over a variety of different families of unsaturated compounds. In particular, the KT-B3LYP calculations correctly predicted the energy ordering of the σ^* and π^* resonances observed in the ET spectra of the (bromoalkyl)ethenes[13] and the empirically scaled π^* VOEs closely reproduced the experimental VAEs.

Here we employ KT-B3LYP/6-31G* and HF/6-31G calculations to characterize the localization properties of the LUMO in bromobenzenes **1**−**5** (Chart 1) and verify whether the π^* VOEs scaled with the appropriate equations reported in the literature[12,21] can supply a good quantitative prediction of the corresponding VAEs measured in the ET spectra.

Experimental Section

Our electron transmission apparatus is in the format devised by Sanche and Schulz[7] and has been previously described.[15] To enhance the visibility of the sharp resonance structures, the impact energy of the electron beam is modulated with a small ac voltage, and the derivative of the electron current transmitted through the gas sample is measured directly by a synchronous lock-in amplifier. Each resonance is characterized by a minimum and a maximum in the derivative signal. The energy of the midpoint between these features is assigned to the VAE. The present spectra were obtained by using the apparatus in the "high-rejection" mode[25] and are, therefore, related to the nearly total scattering cross section. The electron beam resolution was about 50 meV (fwhm). The energy scale was calibrated with reference to the $(1s^12s^2)$ ^2S anion state of He. The estimated accuracy is ± 0.05 or ± 0.1 eV, depending on the number of decimal digits reported.

The collision chamber of the ETS apparatus has been modified[26] to allow for ion extraction at 90° with respect to the electron beam direction. These ions are then accelerated and

focused toward the entrance of a quadrupole mass filter. Alternatively, the total anion current can be collected and measured (with a picoammeter) at the walls of the collision chamber (about 0.8 cm from the electron beam). Although the negative ion current at the walls of the collision chamber can, in principle, be affected by spurious trapped electrons, these measurements are more reliable with respect to the current detected through the mass filter because of kinetic energy discrimination in the anion extraction efficiency in the latter. In a previous test[27] with (monochloro)alkanes our relative total anion currents reproduced to within 1% the ratios in the absolute cross sections reported by Pearl and Burrow.[28]

The DEAS data reported here were obtained with an electron beam current more than twice as large as that used for the ET experiment. The energy spread of the electron beam increased to about 120 meV, as evaluated from the width of the SF_6^- signal at zero energy used for calibration of the energy scales.

The relative total anion currents were evaluated from the peak heights, normalized to the same electron beam current and sample pressure (measured in the main vacuum chamber by means of a cold cathode ionization gauge) for all compounds. Preliminary measurements showed that the total anion current reading is linearly proportional to the pressure, at least in the $10^{-5}-4 \times 10^{-5}$ mbar range.

The calculations were carried out with the Gaussian 98 set of programs.[29] The geometry optimizations and electronic structure calculations on the neutral molecules were performed using the B3LYP density functional method[30] with the standard 6-31G* basis set. The calculated VAEs were obtained as the difference between the total energy of the neutral and that of the lowest anion state, both in the optimized geometry of the neutral state.

All the compounds were commercially available.

Results and Discussion

The total energies of the most stable geometries of the neutral molecules were obtained with B3LYP/6-31G* and HF/6-31G calculations. In bromobenzene (**1**), for symmetry reasons, π^*/σ^*_{C-Br} mixing cannot occur in the rigid structure of the neutral molecule and relies on vibronic coupling or geometrical distortion of the anion on the time scale of the π^* resonance. An important structural parameter in the $C_6H_5(CH_2)_nBr$ series is the conformation. The crucial requirement for the occurrence of maximum π^*/σ^*_{C-Br} mixing (the π^* and σ^* labels are used in a local sense) in benzyl bromide (**2**) is that the C−Br bond (adjacent to the π-system) lies in the plane perpendicular to the ring. According to both the HF and B3LYP calculations, the dihedral angle determined by the ring and the C−Br bond is close to 90°. Similarly, in 1-Br-2-phenylethane (**3**) and 1-Br-3-phenylpropane (**4**) the first $C(H_2)-C(H_2)$ bond of the alkyl chain must lie in the plane perpendicular to the ring for maximum π^*/σ^*_{C-Br} coupling to occur. According to the calculations in compounds **3** and **4** this dihedral angle is also very close to 90°.

The geometrical parameter which most directly affects the energy of the empty σ^*_{C-Br} MO is the C−Br bond length. This distance is calculated to be nearly constant (B3LYP = 1.99 ± 0.01 Å, HF = 2.02 ± 0.01 Å) in compounds **2**−**4**, whereas according to both methods the C−Br bond length is significantly (0.08 Å) shorter in bromobenzene, where the bromine atom is attached to the ring. Other conditions being the same, this factor would lead to a relative destabilization of the (antibonding) empty σ^*_{C-Br} MO of bromobenzene.

ET Spectra. Figure 1 reports the ET spectra in the 0−6 eV energy range of bromobenzene (**1**), benzyl bromide (**2**), 1-Br-2-phenylethane (**3**), 1-Br-2-phenylpropane (**4**), and 1-bromo-4-chlorobenzene (**5**). The vertical electron attachment energies (VAEs) measured in the ET spectra are given in Table 1.

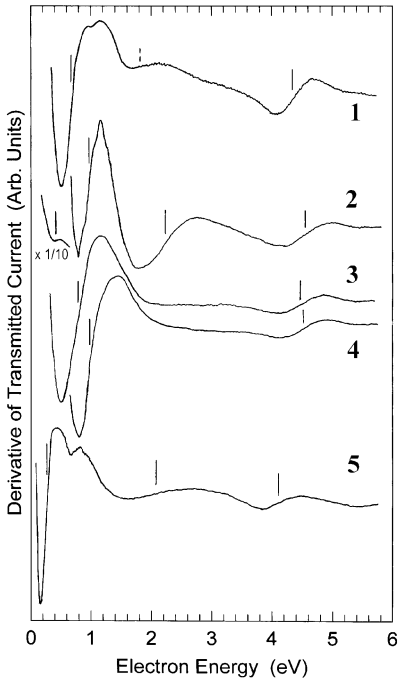

Figure 1. Derivative of transmitted current, as a function of the incident electron energy, in bromobenzene (**1**), benzyl bromide (**2**), 1-Br-2-phenylethane (**3**), 1-Br-3-phenylpropane (**4**), and 1-Br-4-Cl-benzene (**5**). Vertical lines locate the VAEs.

In bromobenzene (C_{2v} point group) the bromine substituent removes the degeneracy of the e_{2u} (π^*) LUMO of benzene (VAE = 1.12 eV[15]) which is split into b_1 (symmetric, with maximum wave function coefficient at the substituted carbon atom) and a_2 (antisymmetric, with a node at the substituted carbon atom) components, here denoted as π^*_S and π^*_A, respectively. The ET spectrum of **1** closely reproduces that previously reported.[31] The low-energy portion of the spectrum displays a large resonance centered at 0.67 eV with a much weaker structure at 1.04 eV. Both the HF/6-31G and the B3LYP/6-31G* calculations predict the π^*_S and π^*_A virtual orbital energies (VOEs) of the neutral state molecule to be essentially equal to each other (see Table 1). Scaling of the VOEs with the empirical linear equations given in the literature[12,21] for the two methods leads to VAEs (in parentheses in Table 1) about 0.2 eV higher than the experimental value of 0.67 eV. The small structure at 1.04 eV is likely to arise from a vibronic interaction between the two π^* anion states, in analogy with the interpretation of the features with similar relative intensities and energy splitting observed in the ET spectra of chlorobenzenes.[32] In particular, a recent combined experimental and theoretical study by Skalicky et al.[33] reveals a dominant role of vibrations of b_2 symmetry in coupling the low-lying b_1 and a_2 π^* anion states of chlorobenzene. Also the VAE (4.35 eV) of the higher lying total antibonding benzene π^* MO (denoted as π^*_O in Table 1) is well reproduced by the scaled VOEs, mainly with the B3LYP calculations. Finally, the weak feature centered at 1.8 eV is associated with electron attachment to the σ^*_{C-Br} MO. However, its narrow width (less than one-half with of the corresponding resonance in linear bromoalkanes[13]) suggests that the low-energy side of this resonance is overlapped and masked by the more intense π^* signal. Assuming that the center of the resonance is shifted to 0.6−0.7 eV lower energy with respect to the maximum in the derivatized signal (as found in the saturated bromides[13])

TABLE 1: Virtual Orbital Energies (VOEs) Supplied by HF/6-31G and B3LYP/6-31G* Calculations and Experimental VAEs[a]

			B3LYP/6-31G*		
cmpd	orbital	HF/6-31G: VOE (scaled)	VOE (scaled)	VAE	expt: VAE (fwhm)
C_6H_6	π^* (b_{2g})	9.942 (5.01)	4.459 (4.80)		4.82
	π^* (e_{2u})	4.030 (1.15)	0.098 (1.29)	2.305	1.12
C_6H_5Br (**1**)	π^*_O	9.433 (4.68)	3.965 (4.40)		4.35 (0.60)
	σ^*_{C-Br}	4.299	0.197		<1.8
	π^*_A	3.522 (0.82)	−0.342 (0.92)		
	π^*_S	3.506 (0.81)	−0.342 (0.92)	1.736	0.67 (0.62)
$C_6H_5CH_2Br$ (**2**)	π^*_O	10.082 (5.10)	4.562 (4.88)		4.55 (0.65)
	$\sigma^*_{C-Br} - \pi^*_S$	4.999 (1.78)	0.827 (1.88)		2.26 (0.95)
	π^*_A	3.677 (0.92)	−0.211 (1.04)		0.97 (0.35)
	$\pi^*_S + \sigma^*_{C-Br}$	2.637 (0.24)	−1.002 (0.40)	0.892	≤0.4 (sh)
$C_6H_5(CH_2)_2Br$	π^*_O	9.284 (4.58)	4.110 (4.52)		4.46 (0.68)
1-Br,2-phenylethane (**3**)	$\sigma^*_{C-Br} - \pi^*_S$	4.621	0.543		
	π^*_A	3.688 (0.93)	−0.175 (1.07)		
	$\pi^*_S + \sigma^*_{C-Br}$	3.244 (0.64)	−0.507 (0.80)	1.249	0.80 (0.65)
$C_6H_5(CH_2)_3Br$	π^*_O	9.555 (4.76)	4.352 (4.72)		4.52 (0.66)
1-Br,3-phenylpropane (**4**)	$\sigma^*_{C-Br} - \pi^*_S$	4.085	0.179		
	π^*_A	3.822 (1.02)	−0.051 (1.17)		
	$\pi^*_S + \sigma^*_{C-Br}$	3.747 (0.97)	−0.147 (1.09)	1.516	0.98 (0.67)
4-Cl-C_6H_5Br (**5**)	π^*_O	8.938 (4.35)	3.517 (4.04)		4.09 (0.53)
	σ^*_{C-Cl}	4.898	0.717		
	σ^*_{C-Br}	3.877	−0.094		2.1 (1.0)
	π^*_S	3.015 (0.49)	−0.713 (0.64)		
	π^*_A	2.998 (0.48)	−0.739 (0.62)	1.270	0.26 (0.19)

[a] Scaled VOEs (see text) in parentheses. All values in eV.

would lead to an estimated value of about 1.5 eV for the σ^*_{C-Br} VAE in bromobenzene.

In benzyl bromide (**2**) strong mixing between the σ^*_{C-Br} and π^*_S MOs causes a large stabilization of the LUMO with respect to the noninteracting π^*_A ring MO. The distinct shoulder (VAE $\leq$ 0.4 eV) observed on the high energy side of the intense electron beam signal (see Figure 1) is ascribed to formation of the first anion state. A representation of the LUMO of the neutral compounds **1**−**4**, as supplied by the B3LYP calculations (the HF results are essentially the same), is reported in Figure 2, and similar localization properties are predicted for the singly occupied MO (SOMO) of the corresponding anions. The corresponding antibonding combinations (not shown) possess similar localization properties, although the σ^*_{C-Br} character is somewhat more pronounced than the benzene π^* character. According to the calculations, the first anion state of **2** possesses about equal π^* ring and σ^*_{C-Br} character.

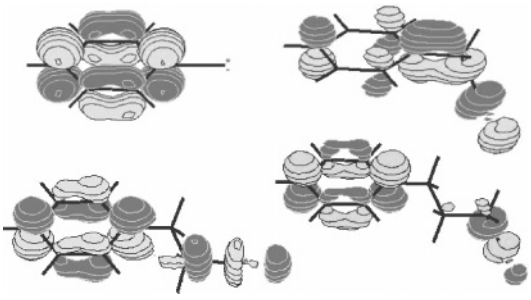

Figure 2. Representation of the LUMO of compounds **1**−**4**, as supplied by B3LYP/6-31G* calculations.

The π^*_A resonance of **2** is located at 0.97 eV and displays vibrational structure with approximate spacing of 130 meV, presumably due, as in benzene, to the ring breathing mode of the anion. Both the HF and B3LYP scaled VOEs accurately reproduce the first two experimental VAEs. The σ^*_{C-Br}/π^*_S antibonding combination, i.e., the out-of-phase counterpart of the LUMO, in line with its large π^* character gives rise to an intense third resonance (VAE = 2.26 eV).

The ET spectra of 1-Br-2-phenylethane (**3**) and 1-Br-2-phenylpropane (**4**) display a single unresolved resonance at low energy (VAE = 0.80 and 0.98 eV in **3** and **4**, respectively) and a resonance at about 4.5 eV associated with the benzene π^*_O MO. For the propyl derivative **4** this result is perfectly consistent with the calculated VOEs, which predict the energy splitting of the two lowest π^* MOs to be less than 0.1 eV (see Table 1) and the σ^*_{C-Br} MO to lie at only 0.3 eV higher energy (so that the σ^* resonance is expected to be hidden by the more intense π^* signal). For the ethyl derivative **3**, the splitting of the two lowest π^* VOEs is calculated to be 0.3 eV and the σ^*_{C-Br} MO to lie about 0.8 eV above the ring π^*_A MO. However, the ET spectrum does not show any distinct σ^* resonance.

According to the calculated localization properties (see Figure 2) the LUMO of $C_6H_5(CH_2)_2Br$ (**3**) possesses about equal ring π^*_S and σ^*_{C-Br} character. A similar nature of the LUMO is also predicted for the chlorine analogue $C_6H_5(CH_2)_2Cl$ and the ethene analogue $H_2C{=}CH(CH_2)_2Br$,[13] although in these cases the energies of the π^* and σ^* MOs (σ^*_{C-Cl} VAE = 2.4 eV in linear chloroalkanes,[34] π^* VAE = 1.73 eV in ethene[14]) are not so close to each other as they are in **3**. As previously pointed out in the literature,[10−12,35] the higher lying intermediate σ^*_{C-C} MOs are inefficient in promoting through-bond coupling of the π^* MO with a remote $\sigma^*_{C-halogen}$ MO. Thus, as hypothesized for $H_2C{=}CH(CH_2)_2Br$,[13] in **3** π^*/σ^* mixing seems more likely to take place directly through space rather than through the intermediate C−C bond.

However, in contrast with $H_2C{=}CH(CH_2)_3Br$, where the LUMO essentially possesses only σ^*_{C-Br} character,[13] and $C_6H_5(CH_2)_3Cl$, where the LUMO essentially possesses only π^*_S character,[11] according to the calculations the LUMO of $C_6H_5(CH_2)_3Br$ (**4**) is about equally localized on the C−Br bond and the benzene ring (see Figure 2). The same result (not shown) is obtained for $C_6H_5(CH_2)_4Br$, where one more CH_2 group separates the two functionals and, of course, through-space interaction cannot occur. This peculiarity of the (bromoalkyl)-benzenes must stem from the close energy proximity of the ring π^* and σ^*_{C-Br} orbitals. However, it is to be noticed that in **4**,

despite its LUMO localization properties, π^*/σ^*_{C-Br} interaction is small, as indicated by the relatively large first VAE and the trend of the calculated π^* and σ^* VOEs along the $C_6H_5(CH_2)_n$-Br series.

Finally, the ET spectrum of 1-Br-4-Cl-benzene (**5**) displays an intense resonance (VAE = 0.26 eV) followed by a narrow and small feature at 0.5 eV higher energy. The electron-withdrawing effect (about 0.9 eV) of the two halogen atoms is nearly additive with respect to those exerted separately in the monohalo derivatives. The second small feature (located at 0.74 eV) is more pronounced than the corresponding signal in brombenzene, but also in this case the first two π^* MOs are calculated to be nearly degenerate in energy (see Table 1), the antisymmetric π^*_A MO being very slightly more stable. The next broad signal is centered at 2.1 eV, i.e., at a somewhat lower energy than the σ^*_{C-Cl} resonance (VAE = 2.42 eV[32]) in chlorobenzene. No distinct σ^*_{C-Br} resonance, calculated to lie at 0.8−1 eV lower energy and presumably superimposed on the descending portion of the π^* signal, is detected.

It can be noticed that the scaled VOEs nicely reproduce the first VAE of compounds **2**−**4**, but that of **1** and **5**, where the halogen atoms are attached directly to the ring, is somewhat overestimated, the maximum error (0.36 eV) occurring in **5** with the B3LYP calculations. This overestimation in **1** and **5** is even more pronounced (see below) when the VAE is calculated as the anion/neutral energy difference.

Table 1 also reports the B3LYP/6-31G* VAEs calculated as the energy difference between the lowest lying anion and the neutral state (both with the optimized geometry of the neutral species). As expected, the calculated VAEs are higher than experimental ones. Moreover, whereas in the series benzene, pyridine, phosphabenzene, and their *tert*-butyl derivatives[22] the calculated and experimental values follow the same energy sequence, in this case the VAE of bromobenzene is predicted to be higher than that of the alkyl derivatives **3** and **4** and the VAE of **5** slightly higher than that of **3**, in contrast with the measured values.

The absolute VAEs calculated with the 6-31+G* basis set which includes diffuse functions are closer to experiment: 1.390 eV (benzene); 0.854 eV (**1**); 0.277 eV (**2**); 0.517 eV (**3**); 0.667 eV (**4**); 0.688 eV (**5**). These values also, however, do not parallel the experimental sequence, the first anion state in **1** and even **5** being more unstable than in **3** and **4**. In addition the SOMO of benzene is described as a diffuse totally symmetric σ^*_{C-H} MO and those of **1**, **4**, and **5** are described as diffuse σ^* MOs with mainly C−Br and ring character. As previously found,[12,22] the present results confirm that it is a hard task to decide a priori which basis set (if any) will be reliable for reproducing the energy and localization properties of unstable anion states, and the numerical agreement with the measured VAE is not the only requirement.

DEA Spectra. Most of the DEA studies reported in the literature are not concerned with the quantitative aspects, i.e., determination of the (absolute or relative) dissociative cross sections. However, quantitative aspects are important and, in particular, for the evaluation of the efficiency of intramolecular electron-transfer processes such measurements become necessary. Our apparatus can measure the total anion current at the walls of the collision chamber or, alternatively, the current of anions extracted from the collision chamber and mass-selected with a quadrupole filter.

Figure 3 displays the total yield of negative ions measured at the collision chamber in compounds **1**−**5**, as a function of the incident electron energy, in the 0−4 eV energy range. Except for **5** (where Cl^- is also present), mass analysis revealed that the total anion current is essentially due only to the Br^- fragment. The energy threshold for Br^- formation is the difference between the C−Br dissociation energy (3.14 eV in 1-Br-propane[36]) and the EA of the bromine atom (3.3636 eV[37]). Although some contribution from traces of impurities cannot be excluded, the zero-energy signals in the DEA spectra are thus associated with the low-energy wing of higher lying resonances, owing to the inverse energy dependence of the electron attachment cross section for the s wave which causes the yield to climb at zero energy.[38] An accurate study of zero-energy cross sections in chloroalkanes has recently appeared in the literature.[39]

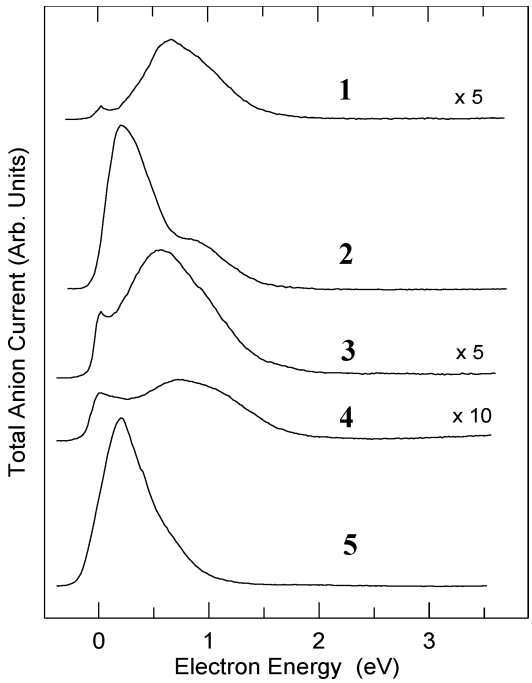

Figure 3. Total anion current, as a function of the incident electron energy, in compounds **1**−**5**.

TABLE 2: Peak Energies (eV), Relative Anion Currents, and Absolute Cross Sections (See Text) Measured in the DEA Spectra of Bromobenzenes 1−5[a]

		DEAS (tot. anion current)		
compd	ETS: VAE	peak energy	int rel to C_6H_5Cl	cross sect (10^{-18} cm^2)
C_6H_5Br (**1**)	0.67	0.66	4.13	128.5
$C_6H_5CH_2Br$ (**2**)	0.97	0.9	12.71	395.4
	≤0.4	0.20	42.39	1318.6
$C_6H_5CH_2CH_2Br$ (**3**)	0.80	0.60	6.61	205.6
$C_6H_5CH_2CH_2CH_2Br$ (**4**)	0.98	0.7	1.59	49.6
4-Cl-C_6H_5Br (**5**)		0.7 (sh)		
	0.26	0.20	43.33	1347.9

[a] The first VAEs (eV) measured in the ET spectra are also reported for comparison.

The peak energies measured in the spectra of compounds **1**−**5** and their intensities relative to chlorobenzene (evaluated from the peak heights under our experimental conditions, with the same electron beam current and the same pressure reading for all the compounds) are given in Table 2. The last column also reports the absolute cross sections as evaluated from comparison of the absolute cross sections found by Burrow and co-workers in chloroalkanes[28] and (chloroalkyl)benzenes[40] with our measurements on the same compounds. The average conversion factor (standard deviation = ±25%) between the two sets of values has been applied to the present bromo derivatives.

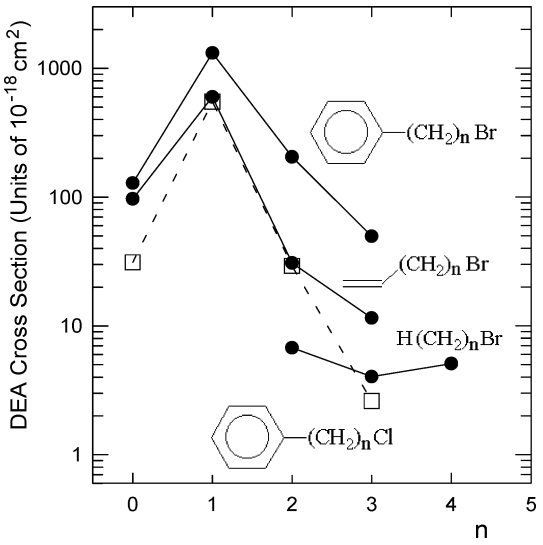

Figure 4. Relative negative ion yields (on a logarithmic scale) in compounds **1**−**4**, the corresponding (chloroalkyl)benzenes (squares), bromoalkenes, and saturated normal bromoalkanes.

The shift to lower energy of the peaks in the DEA spectra with respect to the corresponding resonances observed in ETS is well understood in terms of shorter lifetime and greater distance to the crossing between the anion and neutral potential curves for the anions formed at the high-energy side of the resonance.[41] This shift can be quite large (for instance, about 1 eV in the 1-Cl-alkanes[34]), depending in an inverse fashion upon the resonance lifetime. In particular, in 1-Br-alkanes and in $H_2C{=}CH(CH_2)_3Br$ (where the LUMO has mainly σ^*_{C-Br} character) the shift of the Br^- peaks relative to the corresponding VAEs is about 0.7 eV.[13] In contrast, in $C_6H_5(CH_2)_nCl$ ($n = 3$, 4), where the LUMO has essentially benzene π^* character, the energy of the DEA peaks is nearly coincident with the corresponding VAEs.[11]

In the present bromides $C_6H_5(CH_2)_nBr$ the maxima of the anion currents are relatively close to the VAEs (see Table 2), the largest difference (0.3 eV) occurring in **4** ($n = 3$). The latter finding is thus consistent with the calculated localization properties, according to which even with $n = 3$ or 4 the LUMO possesses about the same σ^*_{C-Br} and π^* ring character, at variance with the LUMO of both the corresponding (bromopropyl)ethene[13] (mainly σ^*_{C-Br}, DEA peak/VAE shift = 0.6 eV) and (chloropropyl)benzene[11] (mainly π^*, DEA peak/VAE shift $\leq$ 0.1 eV).

Figure 4 compares (on a logarithmic scale) the DEA cross sections measured in compounds **1**−**4** with those of the corresponding (bromoalkyl)ethenes and some saturated 1-Br-alkanes.[13] As expected, the largest cross section is found for benzyl bromide (**2**, $n = 1$), where the maximum σ^*_{C-Br}/π^* mixing occurs and the VAE is the smallest. The intensity is 2.2 times larger than that of the ethene analogue allyl bromide[13] and 2.4 times larger than that of the chlorine analogue benzyl chloride.[10] The DEA spectrum of **2** displays a second pronounced maximum at 0.9 eV, close in energy to the π^*_A VAE (0.97 eV) measured in the ET spectrum. A feature (although overlapped to the first more intense signal) at the same energy is also observed in the DEA spectrum of benzyl chloride[10,42,43] but not in the ethene analogues allyl chloride[12,42,43] and bromide.[13] In addition, although the π^*_A MO is essentially localized only on the benzene ring, the DEA spectra of 4-haloanisoles and 4-halopyridines[26] display maxima in the halogen anion yield close in energy to the first π^*_A resonance. Thus, the maximum at 0.9 eV in the DEA spectrum of **2** should be associated with the second (π^*_A) resonance, although contribution from the low-energy side of the third resonance (the antibonding counterpart of the first resonance) cannot a priori be excluded.

The negative current of the (bromoalkyl)benzenes relative to that of the (bromoalkyl)ethenes or the (chloroalkyl)benzenes increases for $n > 1$. In fact, in the order from benzyl bromide ($n = 1$) to 1-Br-3-phenylpropane ($n = 3$) the DEA cross section decrease (about 27 times lower; see Table 2) is relatively small compared to that found on going from $n = 1$ to $n = 3$ in the corresponding (bromoalkyl)ethenes (52 times[13]) and (chloroalkyl)benzenes (>200 times[11]). Inspection of the VAEs (which affect the anion lifetimes in an inverse fashion) does not account for these findings, whereas they are consistent with the different localization properties supplied by the calculations for the SOMO (as well as the LUMO) of the compounds with $n = 3$ in the three series of halides. The first anion state of $C_6H_5(CH_2)_3Br$ has a large C−Br antibonding character but also a relatively long lifetime owing to its large ring π^* character. Consistently, the Br^- yield is 1 order of magnitude larger than that of the saturated normal bromoalkanes. The SOMO of $H_2C{=}CH(CH_2)_3Br$ is mainly a σ^*_{C-Br} MO, and the DEA cross section is of the same order of magnitude as that of the normal bromoalkanes. The SOMO of $C_6H_5(CH_2)_3Cl$ is essentially a ring π^* MO, poorly coupled with the σ (C−Cl) bond where dissociation takes place. Nevertheless, the Cl^- yield is 1 order of magnitude larger than in 1-Cl-butane.[11] In this case the main dissociation mechanism can be thought of as electron attachment to a ring π^* MO followed by intramolecular electron transfer to the opposite end of the molecule through the saturated chain. In contrast, the calculated localization properties suggest that in the bromine analogue $C_6H_5(CH_2)_3Br$ the Br^- current mainly derives from direct dissociation through a resonance with large σ^*_{C-Br} character, although its ring π^* character plays an important role in increasing the resonance lifetime.

Interestingly, despite of the complications due to solvent effects, the rates of dehalogenation of radical anions of nitrobenzyl halides and haloacetophenones measured[45] in the liquid phase using a pulse radiolysis tecnique parallel the trend observed in the gas phase when bromo and chloro derivatives are compared.

Finally, in 1-bromo-4-chlorobenzene (**5**) a total anion current 10 times larger than that of bromobenzene (**1**) and as large as that of benzyl bromide (**2**) was measured (see Table 2). This finding is somewhat unexpected on the basis of the absence of σ^*/π^* interaction (except for vibronic coupling) in **5**, as opposed to the maximum σ^*/π^* mixing in **2**. A plausible explanation can be traced back to a long lifetime of the first resonance of **5**, due to its π^* character and small VAE. The dissociative cross section increases exponentially with the lifetime of the temporary molecular anion.[41] In turn, the lifetime (among other factors) depends in an inverse fashion upon the resonance energy.[44] In addition, ring distortions induced by occupation of the π^* MO could also play some role.

The ratio between the Br^- and the Cl^- currents measured in bromobenzene and chlorobenzene is about 4 (see Table 2). Mass analysis revealed that in **5** the Br^- current peaks at 0.20 eV and is about 20 times more intense than the Cl^- current (peaking at 0.3 eV), with a sizable relative increase in the Br^- yield with respect to the individual monohalobenzenes.

The total anion yield measured in **5** peaks at 0.20 eV and also displays a shoulder at 0.7 eV (see Figure 3), i.e., close in energy to the small and narrow second feature observed in the

ET spectrum. A similar shoulder is also present in the Br^- current selected through a quadrupole mass filter (not shown). As discussed above, the first two π^* anion states of **5** are calculated to be very close in energy to each other. The negative ion current at 0.7 eV could thus be associated with a vibrationally excited π^* anion state. In addition, the energy of this signal (about the same as that of the maxima observed in the saturated bromides[13]) is also consistent with a possible contribution from direct dissociation through the σ^*_{C-Br} resonance.

Conclusions

In this work, we have shown the connection between DEA cross section (peak energy and magnitude) and the empty level structure of bromobenzene, 4-Cl-1-Br-benzene and (bromoalkyl)benzenes, where the π-system and the halogen atom are separated by an alkyl chain.

The neutral state virtual orbital energies supplied by HF/6-31G and B3LYP/6-31G* calculations, scaled with empirical linear equations, satisfactorily reproduce the experimental π^* VAEs measured in the ET spectra. The first VAEs have also been calculated as the energy difference between the lowest lying anion state and the neutral state (both with the optimized geometry of the neutral molecule) with the 6-31+G* basis set which includes diffuse functions. Except for 4-Cl-1-Br-benzene the calculated values are relatively close to experiment, but in some cases the SOMO is described as a diffuse σ^* MO rather than a valence MO with large ring π^* character.

According to the HF/6-31G and B3LYP/6-31G* calculations the LUMO of the (bromoalkyl)benzenes $C_6H_5(CH_2)_nBr$ with $n > 2$ possess localization properties (about equal benzene π^* and σ^*_{C-Br} character) intermediate between those of the corresponding chlorides (with mainly π^* character) and the (bromoalkyl)ethenes $H_2C{=}CH(CH_2)_nBr$ (with mainly σ^*_{C-Br} character). Consistently, in $C_6H_5(CH_2)_3Br$ the shift (0.3 eV) to lower energy of the DEA peak relative to the VAE is intermediate between those found in $C_6H_5(CH_2)_3Cl$ ($\leq$0.1 eV) and $H_2C{=}CH(CH_2)_3Br$ (about 0.6 eV).

Thus, whereas in the (chloroalkyl)benzenes production of Cl^- through dissociation of the first resonance mainly relies upon electron capture into the π ring and subsequent intramolecular electron transfer to the opposite end of the molecule, this mechanism should be less important in the bromides where the extra electron is largely localized also on the C−Br bond. In agreement the DEA cross section of benzyl bromide is 2.4 times larger than that of benzyl chloride, but the ratio (7 for $n = 2$, 19 for $n = 3$) rapidly increases with increasing length of the alkyl chain.

Owing to a strong electron withdrawing inductive effect of the two halogen atoms directly attached to the ring, the first VAE of 1-bromo-4-chlorobenzene is even smaller than that of benzyl bromide, and despite the absence of π^*/σ^* mixing in the equilibrium planar structure of the neutral molecule, the DEA cross section is of the same magnitude, i.e., more than 10 times as large as that of bromobenzene. This indicates that the lifetime of the first vertical anion state is sufficiently long to allow for efficient vibronic coupling and/or geometrical distortion induced by occupation of the LUMO.

Acknowledgment. A.M. thanks the Italian Ministero dell'Istruzione, dell'Università e della Ricerca, and the University of Bologna (Funds for Selected Topics) for financial support.

References and Notes

(1) Massey, H. S. W., McDaniel, E. W., Bederson, B., Eds. *Applied Atomic Collision Physics*; Academic Press: New York, 1984; Vols. 1−5.
(2) Costentin, C.; Robert, M.; Savéant, J.-M. *J. Am. Chem. Soc.* **2004**, *126*, 16834.
(3) Savéant, J.-M. *Acc. Chem. Res.* **1993**, *23*, 455.
(4) Antonello, S.; Maran, F. *Chem. Soc. Rev.* **2005**, *34*, 418.
(5) Schulz, G. J. *Rev. Mod. Phys.* **1973**, *45*, 378, 423.
(6) O'Malley, T. F. *Phys. Rev.* **1966**, *150*, 14.
(7) Sanche, L.; Schulz, G. J. *Phys. Rev. A* **1972**, *5*, 1672.
(8) Illenberger, E.; Momigny, J. *Gaseous Molecular Ions. An Introduction to Elementary Processes Induced by Ionization*; Steinkopff Verlag Darmstadt, Springer-Verlag: New York, 1992.
(9) Ward, M. D. *Chem. Soc. Rev.* **1995**, *24*, 121.
(10) Modelli, A.; Venuti, M. *J. Phys. Chem. A* **2001**, *105*, 5836.
(11) Modelli, A.; Venuti, M.; Szepes, L. *J. Am. Chem. Soc.* **2002**, *124*, 8498.
(12) Modelli, A. *Phys. Chem. Chem. Phys.* **2003**, *5*, 2923.
(13) Modelli, A.; Jones, D. *J. Phys. Chem. A* **2004**, *108*, 417.
(14) Burrow, P. D.; Modelli, A.; Chiu, N. S. *Chem. Phys. Lett.* **1981**, *82*, 270.
(15) Modelli, A.; Jones, D.; Distefano, G. *Chem. Phys. Lett.* **1982**, *86*, 434.
(16) Lane, N. F. *Rev. Mod. Phys.* **1980**, *52*, 29.
(17) Guerra, M. *Chem. Phys. Lett.* **1990**, *167*, 315.
(18) Hehre, W. J.; Radom, L.; Schleyer, P. v. R.; Pople, J. A. *Ab initio Molecular Orbital Theory*; Wiley: New York, 1986.
(19) Dunning, T. H., Jr.; Peterson, K. A.; Woon, D. E. Basis Sets: Correlation Consistent Sets. In *Encyclopedia of Computational Chemistry*; Schleyer, P. v. R., Ed.; John Wiley: Chichester, U.K., 1998.
(20) Heinrich, N.; Koch, W.; Frenking, G. *Chem. Phys. Lett.* **1986**, *124*, 20.
(21) Staley, S. S.; Strnad, J. T. *J. Phys. Chem.* **1994**, *98*, 161.
(22) Modelli, A.; Hajgató, B.; Nixon, J. F.; Nyulászi, L. *J. Phys. Chem. A* **2004**, *108*, 7440.
(23) Koopmans, T. *Physica (Amsterdam)* **1934**, *1*, 104.
(24) Chen, D. A.; Gallup, G. A. *J. Chem. Phys.* **1990**, *93*, 8893.
(25) Johnston, A. R.; Burrow, P. D. *J. Electron Spectrosc. Relat. Phenom.* **1982**, *25*, 119.
(26) Modelli, A.; Foffani, A.; Scagnolari, F.; Jones, D. *Chem. Phys. Lett.* **1989**, *163*, 269.
(27) Modelli, A.; Guerra, M.; Jones, D.; Distefano, G.; Tronc, M. *J. Chem. Phys.* **1998**, *108*, 9004.
(28) Pearl, D. M.; Burrow, P. D. *J. Chem. Phys.* **1994**, *101*, 2940. Aflatooni, K.; Burrow, P. D. *J. Chem. Phys.* **2000**, *96*, 1455.
(29) Frisch, M. J.; Trucks, G. W.; Schlegel, H. B.; Scuseria, G. E.; Robb, M. A.; Cheeseman, J. R.; Zakrzewski, V. G.; Montgomery, J. A., Jr.; Stratmann, R. E.; Burant, J. C.; Dapprich, S.; Millam, J. M.; Daniels, A. D.; Kudin, K. N.; Strain, M. C.; Farkas, O.; Tomasi, J.; Barone, V.; Cossi, M.; Cammi, R.; Mennucci, B.; Pomelli, C.; Adamo, C.; Clifford, S.; Ochterski, J.; Petersson, G. A.; Ayala, P. Y.; Cui, Q.; Morokuma, K.; Malick, D. K.; Rabuck, A. D.; Raghavachari, K.; Foresman, J. B.; Cioslowski, J.; Ortiz, J. V.; Stefanov, B. B.; Liu, G.; Liashenko, A.; Piskorz, P.; Komaromi, I.; Gomperts, R.; Martin, R. L.; Fox, D. J.; Keith, T.; Al-Laham, M. A.; Peng, C. Y.; Nanayakkara, A.; Gonzalez, C.; Challacombe, M.; Gill, P. M. W.; Johnson, B. G.; Chen, W.; Wong, M. W.; Andres, J. L.; Head-Gordon, M.; Replogle, E. S.; Pople, J. A. *Gaussian 98*, revision A.6; Gaussian, Inc.: Pittsburgh, PA, 1998.
(30) Becke, A. D. *J. Chem. Phys.* **1993**, *98*, 5648.
(31) Olthoff, J. K.; Tossell, J. A.; Moore, J. H. *J. Chem. Phys.* **1985**, *83*, 5627.
(32) Burrow, P. D.; Modelli, A.; Jordan, K. D. *Chem. Phys. Lett.* **1986**, *132*, 441.
(33) Skalicky, T.; Chollòet, C.; Pasquier, N.; Allan, M. *Phys. Chem. Chem. Phys.* **2002**, *4*, 3583.
(34) Guerra, M.; Jones, D.; Distefano, G.; Scagnolari, F.; Modelli, A. *J. Chem. Phys.* **1991**, *94*, 484.
(35) Underwood-Lemons, T.; Saghi-Szabo, G.; Tossell, J. A.; Moore, J. H. *J. Chem. Phys.* **1996**, *105*, 7896.
(36) Chen, E. C. M.; Albyn, K.; Dussack, L.; Wentworth, W. E. *J. Phys. Chem.* **1989**, *93*, 6827.
(37) Blondel, C.; Cacciani, P.; Delsart, C.; Trainham, R. *Phys. Rev. A* **1989**, *40*, 3698.
(38) Chutjian, A.; Alajajian, S. H. *Phys. Rev. A* **1985**, *31*, 2885.
(39) Gallup, G. A.; Aflatooni, K.; Burrow, P. D. *J. Chem. Phys.* **2003**, *118*, 2562.
(40) Burrow, P. D. Private communication.
(41) O'Malley, T. F. *Phys. Rev.* **1966**, *150*, 14.
(42) Stricklett, K. L.; Chiu, S. C.; Burrow, P. D. *Chem. Phys. Lett.* **1986**, *131*, 279.
(43) Dressler, R.; Allan, M.; Haselbach, E. *Chimia* **1985**, *39*, 385.
(44) Aflatooni, K.; Burrow, P. D. *Int. J. Mass Spectrom.* **2001**, *205*, 149.
(45) Meot-Ner, M.; Neta, P.; Norris, R. K.; Wilson, K. *J. Phys. Chem.* **1986**, *90*, 168.